International Journal of Mechanical, Industrial and Aerospace Sciences
ISSN: 2517-9950
Vol:5, No:7, 2011

Modeling Strategy and Numerical Validation of the Turbulent Flow over a two-Dimensional Flat Roof

Marco Raciti Castelli, Alberto Castelli, Ernesto Benini

***Abstract*—**The construction of a civil structure inside a urban area inevitably modifies the outdoor microclimate at the building site. Wind speed, wind direction, air pollution, driving rain, radiation and daylight are some of the main physical aspects that are subjected to the major changes. The quantitative amount of these modifications depends on the shape, size and orientation of the building and on its interaction with the surrounding environment.The flow field over a flat roof model building has been numerically investigated in order to determine two-dimensional CFD guidelines for the calculation of the turbulent flow over a structure immersed in an atmospheric boundary layer. To this purpose, a complete validation campaign has been performed through a systematic comparison of numerical simulations with wind tunnel experimental data.Several turbulence models and spatial node distributions have been tested for five different vertical positions, respectively from the upstream leading edge to the downstream bottom edge of the analyzed model. Flow field characteristics in the neighborhood of the building model have been numerically investigated, allowing a quantification of the capabilities of the CFD code to predict the flow separation and the extension of the recirculation regions.The proposed calculations have allowed the development of a preliminary procedure to be used as a guidance in selecting the appropriate grid configuration and corresponding turbulence model for the prediction of the flow field over a two-dimensional roof architecture dominated by flow separation.

***Keywords*—** CFD, roof, building, wind.

I. Introduction And Background

THE construction of a civil structure inevitably changes the outdoor microclimate at the building site. Wind speed, wind direction, air pollution, driving rain, radiation and daylight are some of the main physical aspects which are subjected to the major changes. The quantitative impact of these modifications depend on the shape, size and orientation of the building and on its interaction with the surrounding environment [1].

The use of commercial CFD packages to calculate the wind flow and resulting action on civil structures has aroused a large credit both in research and academic communities as well as in consulting engineering societies, thanks to their capability of providing an insight into the flow field around the buildings even before their construction. Nevertheless, several questions relating to the quality and trust of the numerical predictions come along with the use of such tools [2]. In fact, despite its widespread use, the prediction accuracy and many factors that might affect simulation results are not yet thoroughly understood [3] and, as reported by Franke et al. [4], the general appraisal of the computational approach for quantitative (and sometimes even qualitative) predictions is expressed as lack of confidence. Many emerging issues - concerning wind loadings on civil engineering under extreme weather conditions, pedestrian comfort, optimal conditions for wind turbines, ventilation and dispersion inside urban areas - still remain to be solved.

As pointed out by Stathopoulos [5], the flow around buildings is still extremely difficult to predict by computational methods, even for simple surrounding environments. However, the testing of scale models in a boundary layer wind tunnel, capable of simulating the main velocity profile and turbulence of the natural wind, has been shown to be a very effective method of prediction by comparison with respective full-scale data. These sort of considerations led to the idea of performing numerical validation tests against experimental atmospheric wind tunnel measurements, in order to clarify ambiguities and develop some practical guidelines for CFD predictions of wind flows around buildings by assessing the influence of various computational variables, such as grid resolution, boundary conditions and selection of turbulence models. A selection of the work of Ozmen et al. [6] was chosen as the reference benchmark for the numerical modeling of the wind flow around a simple rectangular building characterized by a flat roof.

As pointed by Dalgliesh [7], roof angle strongly affects the flow around a low-rise building: the flow field over a flat roof model building is dominated by flow separation. The capability of several turbulence models to predict the separation that occurs in the upstream sector of the roof and the extension of the relative recirculation region has been tested for five different vertical longitudinal positions, respectively from the upstream leading edge to the downstream bottom edge of the analyzed model. Also spatial node distribution has been investigated, in order to determine the best compromise between numerical prediction accuracy and computational effort.

Marco Raciti Castelli is Research Associate at the Department of Mechanical Engineering of the University of Padua, Via Venezia 1, 35131 Padova, Italy (e-mail: marco.raciticastelli@unipd.it).

Alberto Castelli is Mechanical Engineering student at the Department of Mechanical Engineering of the University of Padua, Via Venezia 1, 35131 Padova, Italy.

Ernesto Benini is Associate Professor at the Department of Mechanical Engineering of the University of Padua, Via Venezia 1, 35131 Padova, Italy (e-mail: ernesto.benini@unipd.it).

II. Model Geometry

The proposed numerical simulations were based upon the measurements performed by Ozmen et al. [6] in the VKI (von Karman Institute) L-2B wind tunnel [8] by using a 1:100 scale model of the BBRI experimental building [9]: by means of the Counihan technique [10], a turbulent boundary layer of 150 mm thickness was reproduced, allowing the experimental investigation of the flow pattern over the building model.The L-2B facility is a low speed, open circuit wind tunnel of the suction type. It incorporates an air inlet, fitted with honeycomb and meshes, a two-dimensional contraction, and several interchangeable test sections of 0.35 m height, 0.35 m width and various lengths from 0.9 m to 2 m, as can be seen from Fig. 1.

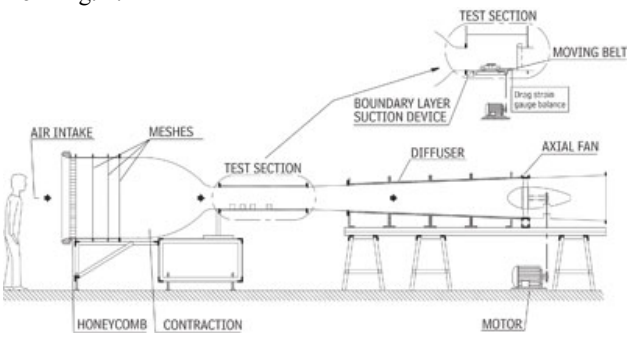

Fig. 1 Schema of the L-2B facility at VKI (from: [11])

In the present work, the flow field inside the wind tunnel was numerically simulated by reproducing a computational domain of rectangular shape, having the same wind tunnel test section size. Table 1 and Fig. 2 summarize the main scale model and test section dimensions.

TABLE I
Main scale model and test section dimensions

$H_{wind\ tunnel}$ [mm]	350
$L_{wind\ tunnel}$ [mm]	1050
L1 [mm]	200
H_{model} [mm]	40
L_{model} [mm]	50
δ [mm]	150
δ /H_{model} [-]	3.75

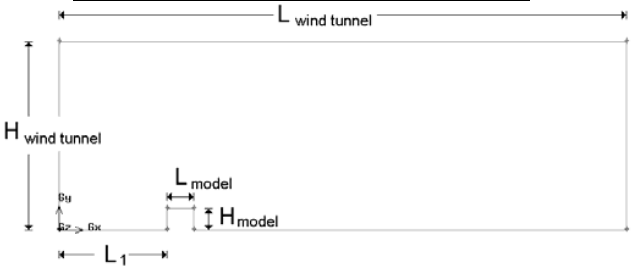

Fig. 2 Main dimensions of the computational model

The numerical model boundary conditions are represented in Fig. 3. Both "*Wall*" and "*Symmetry*" boundary conditions were adopted for the upper portion of the computational domain, and their influence on the numerical results proved completely negligible.

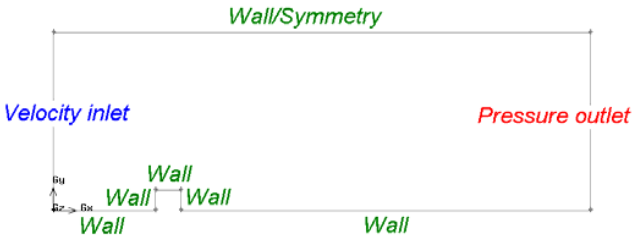

Fig. 3 Boundary conditions of the computational model

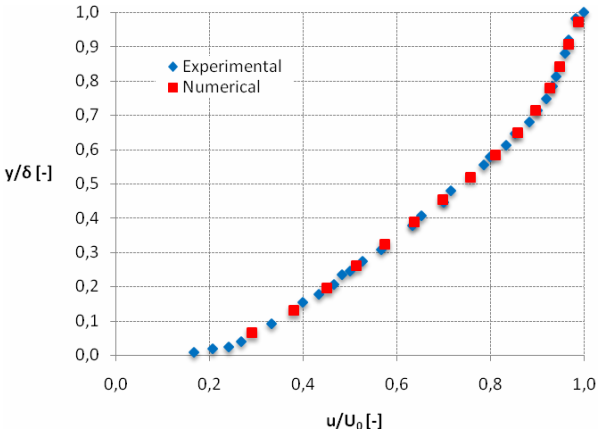

Fig. 4 Comparison between the boundary layer mean horizontal velocity profile obtained by Ozmen et al. [6] and the one adopted in the numerical calculations (the mean horizontal velocity profile was normalized with respect to the reference velocity along the horizontal axis, assumed 15 m/s)

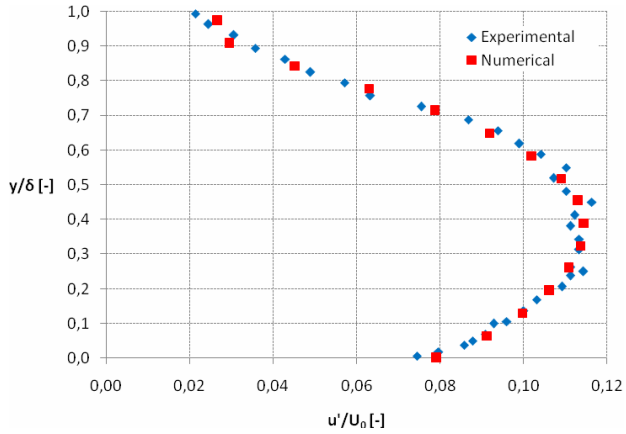

Fig. 5 Comparison between the boundary layer turbulence intensity profile obtained by Ozmen et al. [6] and the one adopted in the numerical calculations

Through the use of proper UDFs (User Defined Functions), the same profiles of the reference boundary layer (in terms of mean velocity and turbulence intensity) obtained by Ozmen et

al. [6] were reproduced in the numerical simulations, as can be seen from Figs. 4 and 5, reporting respectively the mean horizontal velocity profile normalized with respect to the reference velocity along the horizontal axis (assumed 15 m/s) and the boundary layer turbulence intensity profile, defined as:

$$I(y) = u'/U_0 \quad (1)$$

where

$$u' = (u'^{2}_{x})^{0.5} \quad (2)$$

The validation procedure was performed through the comparison of numerical and experimental measurements of the vertical profiles of the x-component mean velocity at five reference positions along the roof length. Fig. 6 shows the displacement of the reference positions, whose normalized x-coordinates with respect to the model building height, defined as:

$$\overline{x} = \frac{x_{\text{reference position}}}{H_{\text{model}}} \quad (3)$$

are reported in Table 2.

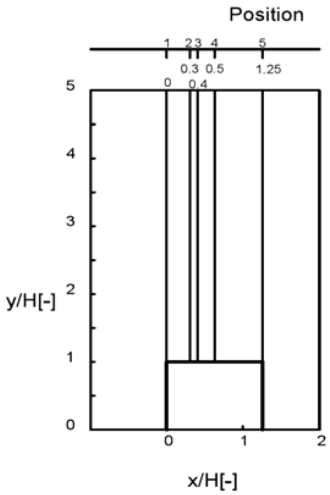

Fig. 6 Displacement of the five reference positions along the roof length that were used for the validation procedure

TABLE II
NORMALIZED X-COORDINATES OF THE FIVE REFERENCE POSITIONS WITH RESPECT TO THE MODEL BUILDING HEIGHT (THE ORIGIN OF THE COORDINATE REFERENCE SYSTEM IS LOCATED AT THE MODEL BUILDING UPSTREAM LEADING EDGE)

Reference position N°	$\overline{x}$ [-]
1	0
2	0.3
3	0.4
4	0.5
5	1.25

III. Spatial Domain Discretization

An isotropic unstructured mesh was created around the model building, in order to test the prediction capability of a very simple grid. Considering their features of flexibility and adaption capability, unstructured meshes are in fact very easy to obtain, for complex geometries, too, and often represent the "first attempt" in order to get a quick response from the CFD in engineering work.

The sensitivity to grid resolution was investigated adopting five different mesh architectures, named *Model_0*, *Model_1*, *Model_2*, *Model_3* and *Model_4*. In Table 3 the characteristic data of the tested grid configurations are reported, as a function of the normalized grid resolution on the model building, defined as:

$$Res_{model} = \Delta g_{model}/H_{model} \quad (4)$$

and as a function of the normalized grid resolution on outer computational domain, defined as:

$$Res_{domain} = \Delta g_{domain}/H_{model} \quad (5)$$

TABLE III
CHARACTERISTIC DATA OF THE TESTED GRID CONFIGURATIONS

Grid name	Res_{model} [-]	Growth factor [-]	Res_{domain} [-]
Model_0	0.25	1.1	2.5
Model_1	0.125	1.1	0.25
Model_2	0.025	1.1	0.25
Model_3	0.0025	1.1	0.25
Model_4	0.0025	1.1	0.025

Figs. from 7 to 9 show a comparison of the main geometrical features of *Model_0*, *Model_2* and *Model_4* grid refinement near the model building, while Fig. 10 displays the whole *Model_2* mesh.

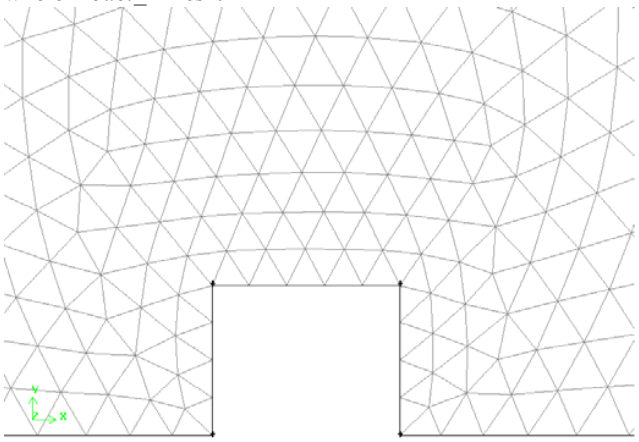

Fig. 7 Main geometrical features of *Model_0* grid refinement near the model building

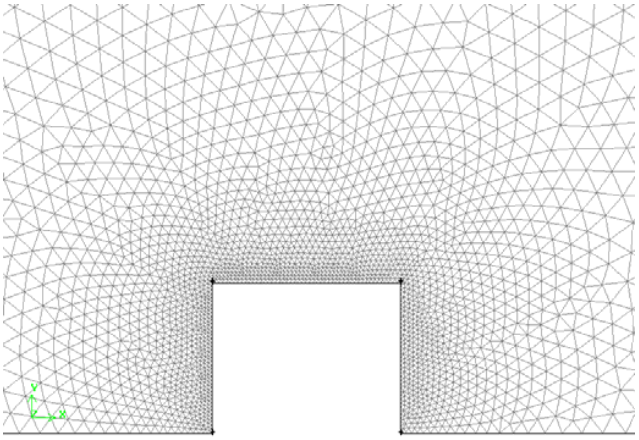

Fig. 8 Main geometrical features of *Model_2* grid refinement near the model building

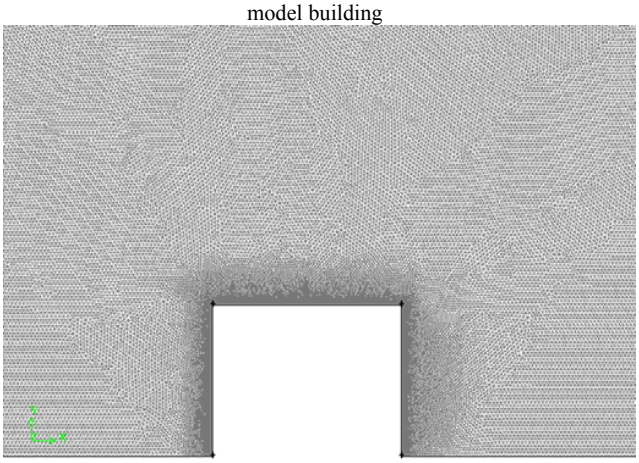

Fig. 9 Main geometrical features of *Model_4* grid refinement near the model building

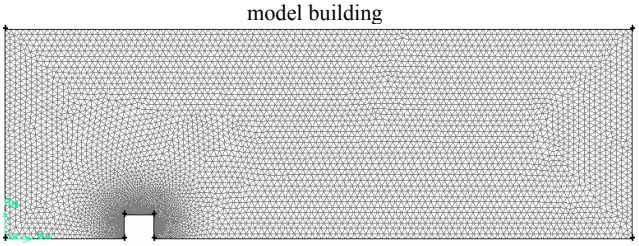

Fig. 10 Main geometrical features of *Model_2* mesh

IV. Turbulence Models and Convergence Criteria

Simulations were performed using the commercial RANS solver ANSYS FLUENT®, which implements 2-D Reynolds-averaged Navier-Stokes equations using a finite volume-finite element based solver. A segregated solver, implicit formulation, was chosen for unsteady flow computation. The fluid was assumed to be incompressible, being the maximum fluid velocity on the order of 16 m/s. As far as the turbulence model is concerned, *Standard k-ε*, *Realizable k-ε* and *k-ω SST* prediction capabilities were tested.

As a global convergence criterion, residuals were set to 10-5. The simulations, performed on a 8 processor, 2.33 GHz clock frequency computer, required a total CPU time from about 1/2 hour (*Model_0*) to more than 3 hours (*Model_4*).

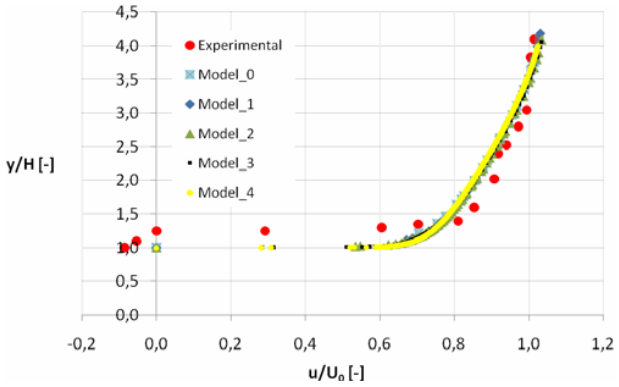

Fig. 11 Comparison between measured and computed x-velocity profiles as a function of grid resolution, *Standard k-ε* turbulence model, reference position N° 1

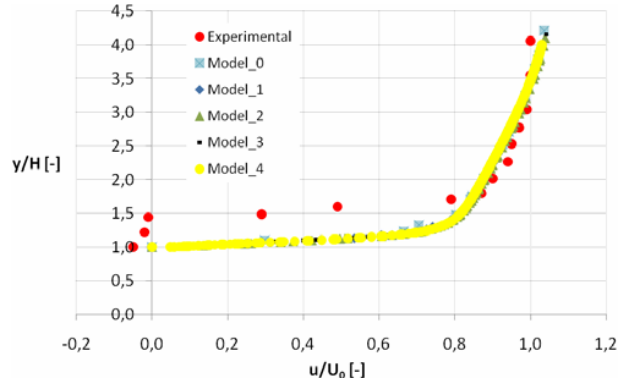

Fig. 12 Comparison between measured and computed x-velocity profiles as a function of grid resolution, *Standard k-ε* turbulence model, reference position N° 2

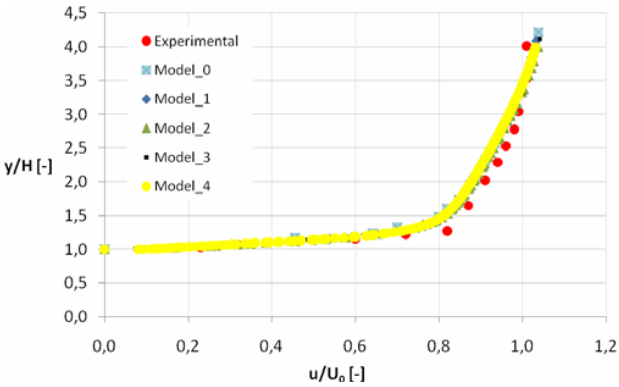

Fig. 13 Comparison between measured and computed x-velocity profiles as a function of grid resolution, *Standard k-ε* turbulence model, reference position N° 3

V. Results And Discussion

Figs. from 11 to 15 represent the comparison between measured and numerically simulated x-velocity profiles as a function of grid resolution for the five reference positions along the roof length and for *Standard k-ε* turbulence model.

The following observations can be drawn:

1. the effect of grid resolution on the computed x-velocity profiles is entirely negligible, being the very same results

obtained by the coarser mesh and the finer one;
2. the numerical code proved to be accurate in predicting the flow-field features close to the model building for reference positions N° 3, 4 and 5, that is after the recirculation region in the upper portion of the model roof;
3. the accuracy in the prediction of the main flow-field characteristics lowers for reference positions N° 1 and 2, that is as the flow separates from the upstream leading edge of the building model, at least close to the model itself.

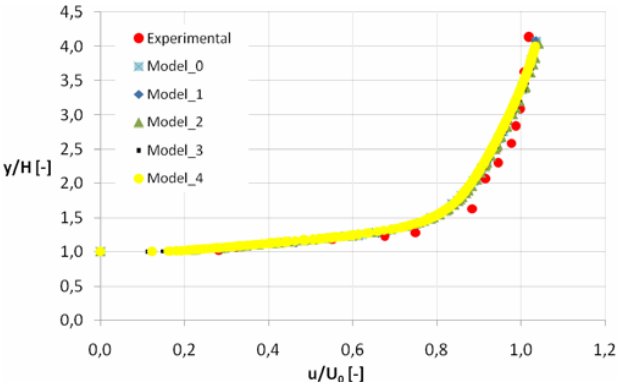

Fig. 14 Comparison between measured and computed x-velocity profiles as a function of grid resolution, *Standard k-ε* turbulence model, reference position N° 4

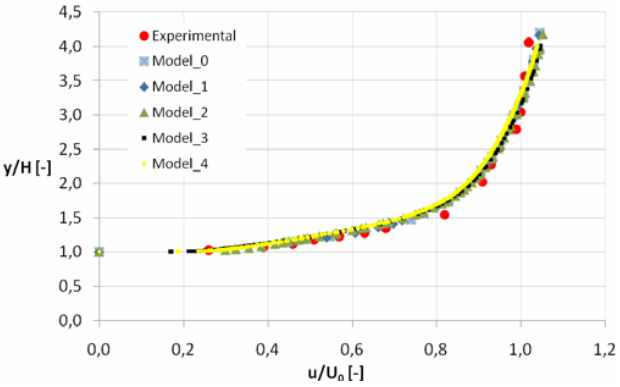

Fig. 15 Comparison between measured and computed x-velocity profiles as a function of grid resolution, *Standard k-ε* turbulence model, reference position N° 5

On the basis of consideration N° 1, mesh *Model_2* was adopted for the choice of the best turbulence model. Figs. from 16 to 20 show the influence of the turbulence model on the accuracy of the numerical predictions.

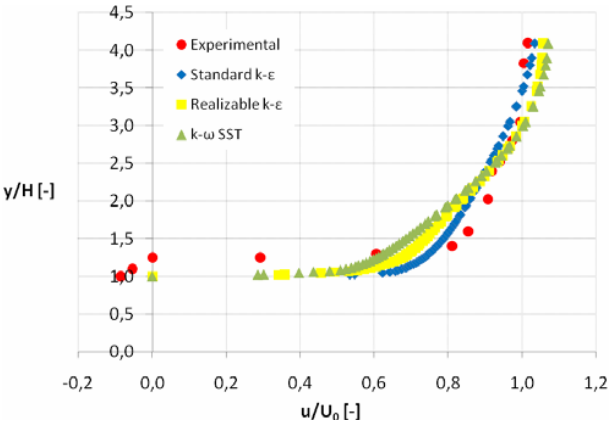

Fig. 17 Influence of the turbulence model on the accuracy of the numerical predictions, *Model_2* mesh, reference position N° 1

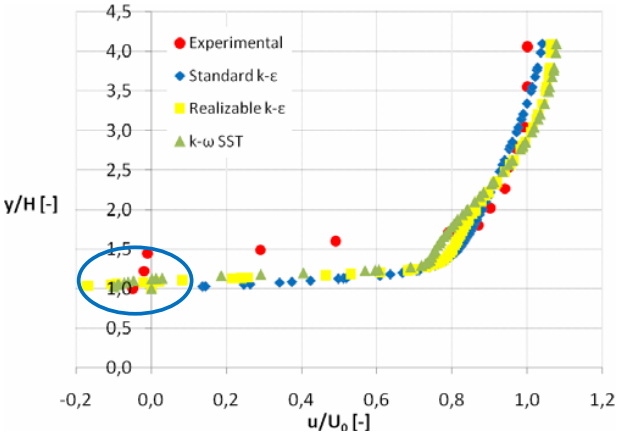

Fig. 17 Influence of the turbulence model on the accuracy of the numerical predictions, *Model_2* mesh, reference position N° 2

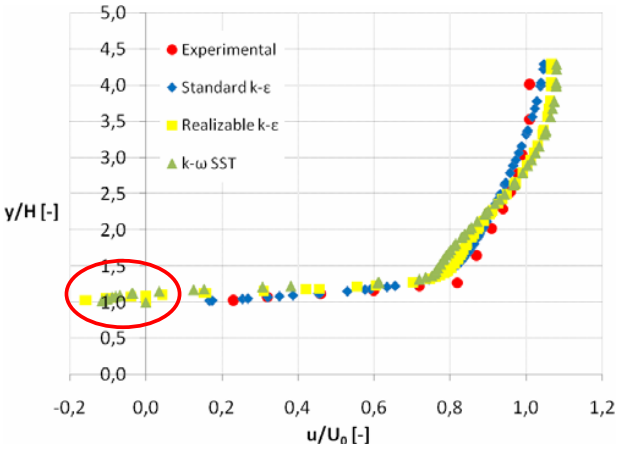

Fig. 18 Influence of the turbulence model on the accuracy of the numerical predictions, *Model_2* mesh, reference position N° 3

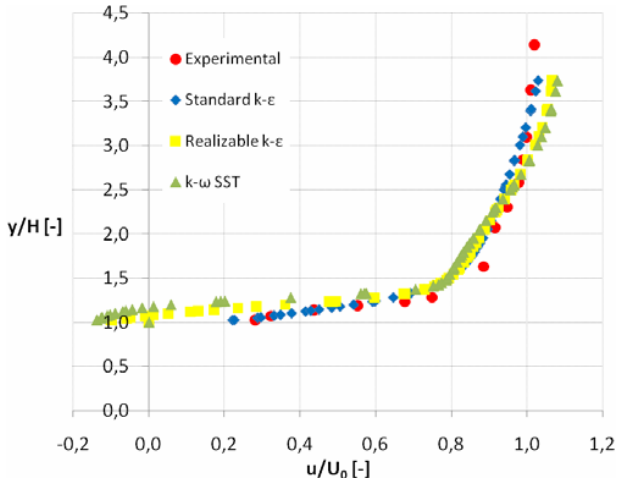

Fig. 19 Influence of the turbulence model on the accuracy of the numerical predictions, *Model_2* mesh, reference position N° 4

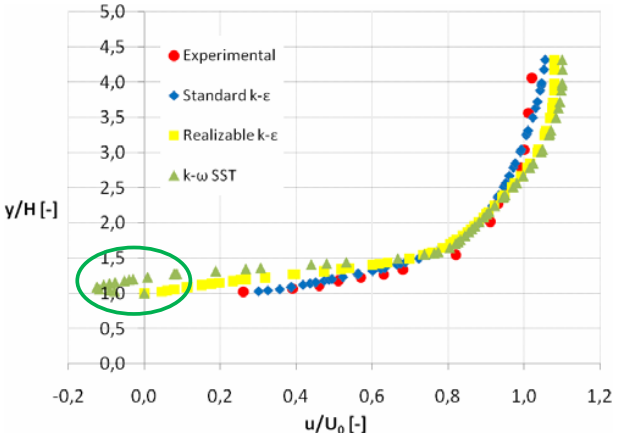

Fig. 20 Influence of the turbulence model on the accuracy of the numerical predictions, *Model_2* mesh, reference position N° 5

As can be clearly seen, *Standard k-ε* prediction capabilities to reproduce the experimental measurements appear to be slightly higher with respect to *Realizable k-ε* and *k-ω SST* turbulence models, both for separated (reference positions N° 1 and 2) and for attached flow conditions (reference positions N° 3, 4 and 5). This is in accordance to the findings of Yoshie et al. [3], which adopted the *Standard k-ε* model for the prediction of the flow-field around a building model.Unlike the *Standard k-ε* model, both *Realizable k-ε* and *k-ω SST* turbulence models were able to correctly predict a recirculation region for reference position N° 2 (evidenced by a blue circle on Fig. 17). Nevertheless, they continued to predict a reverse flow also for reference positions N° 3 and 4 (evidenced by a red circle on Figs. 18 and 19), which is in contrast to the experimental measurements. Moreover, *k-ω SST* turbulence model predicts a recirculation region even for reference position N° 5 (evidenced by a green circle on Fig. 20), which is totally in contrast with the experimental measurements.

Figs. 21 and 22 represent the contours of absolute velocity on the top of the roof respectively for *Standard k-ε* and *k-ω SST* models. As can be clearly seen, the computed recirculation region is much bigger for *k-ω SST* with respect to the *Standard k-ε* model.

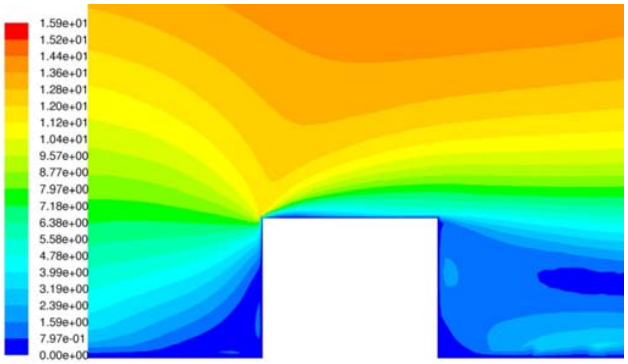

Fig. 21 Contours of absolute velocity on the top of the roof for *Standard k-ε* turbulence model

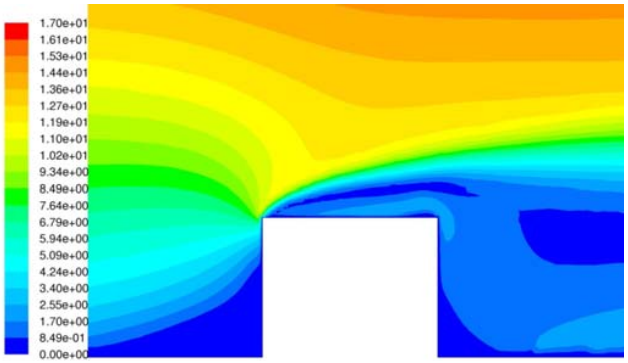

Fig. 22 Contours of absolute velocity on the top of the roof for *k-ω SST* turbulence model

VI. Conclusions and Future Works

In the present work numerical validation tests were performed against experimental atmospheric wind tunnel measurements, in order to develop some practical guidelines for CFD predictions of wind flows around buildings by assessing the influence of various computational variables, such as grid resolution, boundary conditions and selection of turbulence models. An experimental case study [6] was chosen as the reference benchmark for the 2D numerical modeling of the wind flow around a simple rectangular building characterized by a flat roof.

The comparison between experimental measurements and numerical predictions proved that the effect of grid resolution on the computed x-velocity profiles is negligible, at least for the tested grid resolutions (ranging from 0.25 to 0.0025 of the model height). Also the influence of the boundary condition adopted for the upper portion of the computational domain (both "*Wall*" and "*Symmetry*") proved to be completely negligible.*Standard k-ε* prediction capabilities to reproduce the experimental measurements appeared to be slightly higher

with respect to *Realizable k-ε* and *k-ω SST* turbulence models, both for separated and for attached flow conditions. Unlike the *Standard k-ε* model, both *Realizable k-ε* and *k-ω SST* turbulence models were able to correctly predict a recirculation region close to the model building leading edge. Nevertheless, they continued to predict a reverse flow also for other portions of the roof, which is in contrast to the experimental measurements.

In conclusion, it can be stated that the numerical code proved to be quite accurate in predicting the flow-field features after the recirculation region in the upper portion of the model roof, while the prediction capabilities lowered close to the upstream leading edge of the building model, in correspondence of the recirculation region.

Further work should be done in order to numerically investigate the 3D effects on the flow field over the flat roof model building, so as to complete the definition of a preliminary procedure to be used as a guidance in selecting the appropriate grid configuration and corresponding turbulence model for the prediction of the flow field over a roof architecture dominated by flow separation.

NOMENCLATURE

H_{model} [mm]	model height
$H_{wind\ tunnel}$ [mm]	wind tunnel test section height
I [-]	turbulence intensity profile
L_1 [mm]	distance between wind tunnel inlet condition and tested model
L_{model} [mm]	model length
$L_{wind\ tunnel}$ [mm]	wind tunnel length
Res_{domain} [-]	normalized grid resolution on outer computational domain
Res_{model} [-]	normalized grid resolution on the model building
u [m/s]	mean velocity along the horizontal axis
u' [m/s]	root-mean-square of the turbulent velocity fluctuation
u_x' [m/s]	turbulent velocity fluctuation along the horizontal axis
U_0 [m/s]	reference velocity along the horizontal axis
$x_{reference\ position}$ [mm]	distance between the scale model upstream leading edge and the reference position for the validation procedure
$\bar{x}$ [-]	normalized x-coordinate of the reference position for the validation procedure with respect to the model building length
y [mm]	coordinate along the vertical axis
δ [mm]	turbulent boundary layer thickness
$δ/H_{model}$ [-]	ratio of boundary layer thickness to model height
$Δg_{domain}$ [mm]	grid resolution on outer computational domain
$Δg_{model}$ [mm]	grid resolution on the model building

ACKNOWLEDGMENT

The present work was sponsored by Epoca S.r.l., Trieste (Italy) in order to develop a numerical model for the prediction of the turbulent flow field around the new Via dei Giustinelli building, Trieste (Italy).

REFERENCES

[1] Blocken, B., Carmeliet, J., *Pedestrian Wind Environment around Buildings: Literature Review and Practical Examples*, Journal of Thermal Envelope and Building Science, Oct 2004, 28: 107-159;

[2] Jensen, A. G., Franke, J., Hirsch, C., Schatzmann, M., Stathopoulos, T., Wisse, J., Wright, N. G., *Impact of Wind and Storm on City Life and Built Environment – Working Group 2 – CFD Techniques – Computational Wind Engineering*, Proceedings of the International Conference on Urban Wind Engineering and Building Aerodynamics, COST Action C14, Von Karman Institute, Rhode-Saint-Genèse, Belgium, May 5-7, 2004;

[3] Yoshie, R., Mochida, A., Tominaga, Y., Kataoka, H., Harimoto, K., Nozu, T., Shirasawa, T., *Cooperative Project for CFD Prediction of Pedestrian Wind Environment in the Architectural Institute of Japan*, Journal of Wind Engineering and Industrial Aerodynamics, 95 (2007) 1551-1578;

[4] Franke, J., Hirsch, C., Jensen, A. G., Krus, H. W., Schatzmann, M., Westbury, P. S., Miles, S. D., Wisse, J. A., Wright, N. G., *Recommendations on the Use of CFD in Wind Engineering*, Proceedings of the International Conference on Urban Wind Engineering and Building Aerodynamics, COST Action C14, Von Karman Institute, Rhode-Saint-Genèse, Belgium, May 5-7, 2004;

[5] Stathopoulos, T., *Wind Effects on People*, Proceedings of the International Conference on Urban Wind Engineering and Building Aerodynamics, COST Action C14, Von Karman Institute, Rhode-Saint-Genèse, Belgium, May 5-7, 2004;

[6] Ozmen, Y., Van Beeck, J. P. A. J., Baydar, E., *The Turbulent Flow over Three Dimensional Roof Modles Immersed in an Atmospheric Boundary Layer*, Proceedings of the International Conference on Urban Wind Engineering and Building Aerodynamics, COST Action C14, Von Karman Institute, Rhode-Saint-Genèse, Belgium, May 5-7, 2004;

[7] Dalgliesh, W. A., *Wind Loads on Low Buildings*, Division of Building Research, National Research Council of Canada, Ottawa, January 1981;

[8] http://www.vki.ac.be/;

[9] Parmentier, B., Hoxey, R., Buchlin, J. M., Corieri, P., *The Assessment of Full Scale Experimental Methods for Measuring Wind Effects on Low Rise Buildings*, COST Action C14, Impact of Wind and Storm on City Life and Built Environment, June 3-4, 2002, Nantes, France;

[10] Counihan, J., *An Improved Method of Simulating an Atmospheric Boundary Layer in a Wind Tunnel*, Atmos. Environ., Vol. 3 (1969), pp. 197-214;

[11] http://www.vki.ac.be/index.php?option=com_content&view=article&id=60:low-speed-wind-tunnel-l-2b&catid=48:low-speed-wind-tunnels&Itemid=151.